Cancer Biol Med 2026. doi: 10.20892/j.issn.2095-3941.2025.0120

ORIGINAL ARTICLE

BEX2 influences the MCL1-Hedgehog signaling axis to regulate the potential of stemness characterization in colorectal cancer

Yucheng Qian[1,2,3,4]*, Jingsun Wei[1,2,3,4]*, Yuan Bian[5]*, Yinuo Tan[2,3,4,6], Yimin Fang[1,2,3,4], Liubo Chen[1,2,3,4], Kai Jiang[1,2,3,4], Dongliang Fu[1,2,3,4], Xiaoxu Ge[1,2,3,4], Tianyi Ling[1,2,3,4], Qian Xiao[1,2,3,4], Kefeng Ding[1,2,3,4], Yeting Hu[1,2,3,4]

[1]Department of Colorectal Surgery and Oncology (Key Laboratory of Cancer Prevention and Intervention, China National Ministry of Education, Key Laboratory of Molecular Biology in Medical Sciences, Zhejiang Province, China), The Second Affiliated Hospital, Zhejiang University School of Medicine, Hangzhou 310000, China; [2]Center for Medical Research and Innovation in Digestive System Tumors, Ministry of Education, Hangzhou 310000, China; [3]Zhejiang Provincial Clinical Research Center for CANCER, Hangzhou 310000, China; [4]Cancer Center of Zhejiang University, Hangzhou 310000, China; [5]Department of Colorectal Surgery, Shaoxing Central Hospital, Shaoxing 312030, China; [6]Department of Medical Oncology, Key Laboratory of Cancer Prevention and Intervention, Ministry of Education, The Second Affiliated Hospital, Zhejiang University School of Medicine, Hangzhou 310009, China

ABSTRACT

Objective: Colorectal cancer (CRC) progression is driven by cancer stem cells (CSCs) that evade treatment through dynamic phenotype modulation. Our previous research identified BEX2 as a significant regulator of CRC malignancy involving the Hedgehog (Hh) pathway. This study aimed to elucidate the influence of BEX2 on CRC stemness and the interaction with the Hh signaling pathway, potentially uncovering innovative therapeutic strategies for combating CRC.

Methods: TCGA and GEO data were analyzed to correlate BEX2 expression with clinical outcomes and stemness markers in CRC. Functional assays, including spheroid formation, flow cytometry, extreme limiting dilution assay (ELDA), Transwell, wound healing, and cell viability assay, were performed in DLD1 and HCT116 cell lines. Immunoblotting and qRT-PCR assessed BEX2 expression with *in vivo* validation in NOD/SCID mice.

Results: The findings revealed a negative correlation between BEX2 expression and the levels of stemness-associated genes with a significant association with CRC patient' prognosis. Overexpression of *BEX2* diminished CRC stemness potential, whereas BEX2 knockdown led to a pronounced enhancement of these stem-like characteristics. Further investigation revealed that BEX2 inhibited the Hh pathway. BEX2 interacted with MCL1, promoting ubiquitination and degradation, thereby decreasing MCL1 stability. Low *BEX2* expression stabilized MCL1, which enhanced stemness potential. These results suggested BEX2 modulates CRC stemness *via* MCL1 downregulation.

Conclusions: Taken together, the current study findings highlight BEX2 and MCL1 as potential therapeutic targets in CRC with BEX2 emerging as a key regulator of stemness, chemoresistance, and invasiveness. These findings advance our understanding of CRC and pave the way for more effective therapies.

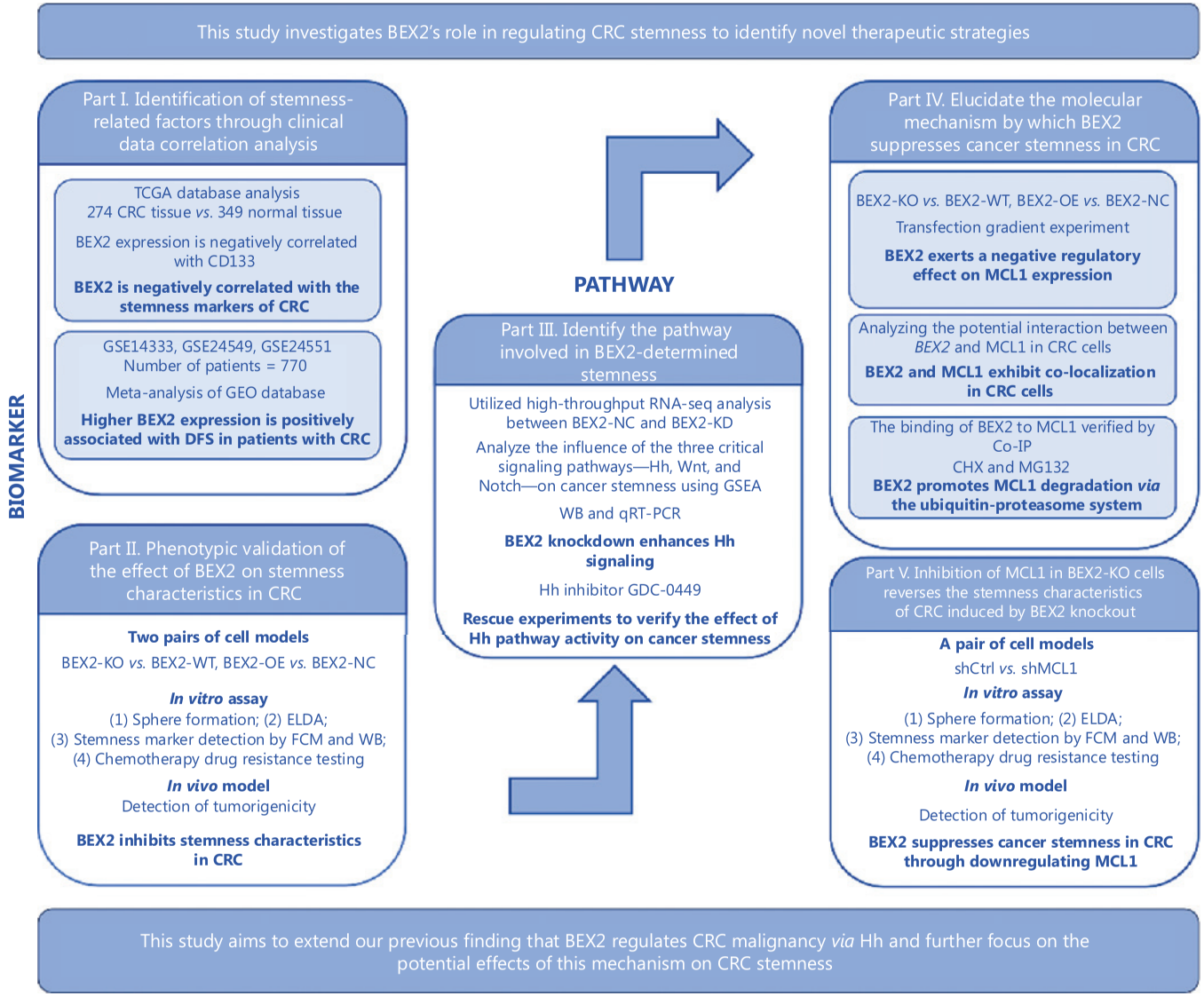
KEYWORDS Cancer stemness; BEX2; MCL1; Hedgehog

Introduction

Colorectal cancer (CRC) is a malignant tumor that is prevalent globally and poses a substantial health challenge[1,2]. Despite advances in treatment, relapse remains a major issue that is largely due to cancer stem cells (CSCs)[3-5]. CSCs exhibit strong self-renewal, resistance to therapy, and can drive tumor heterogeneity and recurrence through high expression of markers, like OCT4, Nanog, EpCAM, and SOX2[6-8].

Dysregulation of the Hedgehog (Hh) pathway is crucial for maintaining stemness, cell fate determination, and

*These authors contributed equally to this work.
Correspondence to: Kefeng Ding and Yeting Hu
E-mail: dingkefeng@zju.edu.cn and huyt@zju.edu.cn
ORCID ID: https://orcid.org/0000-0002-2380-3717 and https://orcid.org/0000-0001-7483-4380
Received March 28, 2025; accepted January 5, 2026.
Available at www.cancerbiomed.org
©2026 The Authors. Creative Commons Attribution-NonCommercial 4.0 International License (CC BY-NC 4.0)



Study flowchat **Part I.** Based on an analysis of the TCGA database, *BEX2* expression was significantly downregulated in CRC tissues compared to normal tissues and a meta-analysis of the GSE14333, GSE24549, and GSE24551 datasets further demonstrated that patients with low *BEX2* expression had a shorter DFS. Correlation analyses utilizing TCGA and GTEx databases revealed a significant negative relationship between *BEX2* expression and stemness markers (CD133 and CD44). **Part II.** *In vitro* functional validation using BEX2-KO and BEX2-OE CRC cell lines demonstrated that BEX2 negatively regulates CRC cell stemness. This conclusion was supported by observations, including expanded CD133+ subpopulations, increased tumorsphere formation, upregulation of NANOG and OCT4, as well as heightened migratory/invasive ability and chemoresistance, all of which were significantly enhanced in the *BEX2* low-expression group. *In vivo* experiments using NOD/SCID mice demonstrated that CRC cells with low *BEX2* expression exhibit enhanced tumorigenicity, as assessed using a tumor cell gradient dilution assay. **Part III.** GSEA

indicated a significant enrichment of the Hh signaling pathway in the *BEX2* low-expression group. This enrichment was observed with other significantly activated pathways. Subsequent molecular validation confirmed substantial upregulation of Hh pathway components, including Gli1, PTCH1, and HHIP, in BEX2-KO DLD1 cells. Conversely, these Hh pathway components were significantly downregulated in BEX2-OE HCT116 cells. These findings were corroborated by WB at the protein level. Furthermore, application of the specific Hh pathway inhibitor, GDC-0449, effectively reversed the enhanced sphere-forming capacity that was induced by low *BEX2* expression. **Part IV.** Functional analyses in BEX2-KO and BEX2-OE CRC cells demonstrated an inverse relationship between BEX2 and MCL1 protein levels, which was validated by immunoblotting. BEX2-MCL1 interaction and cytoplasmic co-localization were confirmed *via* co-immunoprecipitation and immunofluorescence. CHX- and MG132-mediated proteasome inhibition assays indicated accelerated MCL1 degradation *via* enhanced ubiquitination. WB identified BEX2 as a recruiter of the E3 ligase, BTRC, facilitating K48-linked polyubiquitination and proteasomal degradation of MCL1 to reduce MCL1 stability. **Part V.** Rescue experiments using the MCL1-specific inhibitor, MIM1, and *MCL1*-targeting shRNA in BEX2-KO cells validated that enhancement of cancer stemness phenotypes upon BEX2 depletion is MCL1-dependent. This conclusion was supported by observations, including expanded CD44+/CD133+ subpopulations, increased tumorsphere formation, upregulation of NANOG and OCT4, as well as heightened migratory/invasive ability and chemoresistance, all of which were markedly attenuated following MCL1 inhibition. *In vivo* experiments using NOD/SCID mice demonstrated that BEX2-KO CRC cells with *MCL1* shRNA exhibited reduced tumorigenicity compared to the control group. CRC, colorectal cancer; Co-IP, Co-immunoprecipitation; TCGA, The Cancer Genome Atlas; GEO, Gene Expression Omnibus; DFS, disease-free survival; FCM, flow cytometry; WB, western blot; Hh, Hedgehog; NC, normal control; KO, knockout; OE, overexpression; WT, wild type; GSEA, Gene Set Enrichment Analysis; CHX, cycloheximide.

self-renewal in CSCs[9-11]. Recent studies have shown that myelogenous leukemia-1 (MCL1) interacts with the Gli inhibitor, SUFU, to block inhibition of Gli1 and thus activating the Hh pathway[12,13]. MCL1 is often aberrantly expressed in malignant tumors[14-16] but the role of MCL1 in the Hh pathway and CSC regulation has not been established.

BEX2, an intrinsically disordered protein, is epigenetically silenced in primary gliomas and re-expression of BEX2 inhibits tumor proliferation[17,18]. Our previous research showed that silencing BEX2 enhances migration and invasion in CRC cells, suggesting a role in regulating tumor malignancy under some conditions[19]. However, the comprehensive role of BEX2 in regulating CRC stemness is unknown.

This study determined the impact of *BEX2* knockdown or overexpression on cancer stemness, Hh signaling, and therapeutic resistance in CRC *in vitro* and *in vivo*. BEX2 was shown to reduce stemness in CRC cell lines by promoting MCL1 degradation and inhibiting the Hh pathway. Conversely, MCL1 enhanced Hh activity and CRC stemness. Inhibiting MCL1 expression counteracted the enhanced stemness in *BEX2* knockdown cells. The findings herein highlight BEX2 as a promising target for CRC therapy.

Materials and methods

Cell culture, transfection, and transduction

Human CRC cell lines (DLD1 and HCT116) were obtained from the American Type Culture Collection [ATCC] (Manassas, VA, USA). These cells were cultured in RPMI-1640 medium (Gibco) supplemented with 10% fetal bovine serum [FBS] (Gibco), 100 U/mL of penicillin, and 100 μg/mL of streptomycin. *BEX2* stable knockout cells (BEX2-KO-DLD1) were established previously[19]. HEK 293 cells, also procured from the ATCC, were cultured in Dulbecco's modified Eagle's medium (Gibco, Carlsbad, CA) with the same supplements.

Transfection was carried out using Lipofectamine 2000 (Invitrogen, Carlsbad, CA). Transduction was performed using lentivirus at a multiplicity of infection of 10. Stable clones were selected with 4 μg/mL of puromycin (Sigma-Aldrich, Beyotime, Hangzhou, China). Constructs were transformed into HEK 293T cells with lentivirus packaging reagents (Addgene, Invitrogen, Carlsbad, CA) following the manufacturer's instructions. The shRNA sequences utilized are listed in **Table S1**.

Establishment of stable *BEX2* overexpression cell lines

BEX2 overexpression in HCT116 cells was achieved using the lentiviral-based vector, pLent-RFP-Blasticidin-CMV (Addgene, Invitrogen, Carlsbad, CA). The lentiviral-based vector, pLKO.1-Puro (Addgene), was utilized for shRNA expression. *BEX2* was amplified and cloned into the pCMV-HA vector (Addgene, Invitrogen, Carlsbad, CA) using a *BEX2* DNA fragment as a template in the transfection of HEK 293 cells. Similarly, MCL1 was amplified using an *MCL1* DNA fragment as a template and cloned into the pCMV-3xflag vector (Addgene, Invitrogen, Carlsbad, CA).

Bioinformatic analyses

Three GEO datasets (GSE14333, GSE24549, and GSE24551) containing patient clinical characteristics and RNA-seq data from colon adenocarcinoma (COAD) tissues were utilized. Pearson's correlation coefficients were used to describe the relationship between BEX2 and disease progression. Normalized RNA-seq data for BEX2, OCT4, NANOG, CD44, and CD133 from the TCGA database (https://portal.gdc.cancer.gov/) were analyzed to assess the correlations in COAD tissues.

Flow cytometry analysis

Cells were harvested and resuspended in PBS containing 2% FBS, then stained with fluorescein Isothiocyanate (FITC)-conjugated CD44 antibody (Biolegend, Shanghai, China) or allophycocyanin (APC)-conjugated CD133 antibody (Biolegend) for 30 min at 4°C in the dark. DAPI (Sigma-Aldrich) was used for dead cell exclusion. Flow cytometry analysis was performed using a Beckman Coulter DxFLEX and data were analyzed using FlowJo software.

Tumor sphere formation assay

Cells (5×10^3 cells per well) were seeded in 6-well ultra-low attachment plates (Corning, NY, USA) in serum-free DMEM/F12 (1:1) medium (Gibco) containing 2% B27 supplement (Gibco), 20 ng/mL human fibroblast growth factor [FGF] (PeproTech, MA, USA), and 20 ng/mL epidermal growth factor [EGF] (PeproTech, MA, USA). Cells were fixed with 4% formaldehyde after 12–14 d and stained with 0.1% crystal violet, followed by photography. Spheres with diameters > 75 μm were counted. Each experiment was performed at least three times.

In vivo xenograft assay

Six-week-old female NOD/SCID mice (SLAC Laboratory Animal Co., Ltd., Shanghai, China) were subcutaneously injected with a total of 1×10^2–1×10^5 DLD1 or HCT116 cells embedded in Matrigel (BD Biosciences, Sigma, MO, USA). Tumor size and weight were evaluated 7 weeks post-injection upon sacrificing the mice. All experiments were performed following the Institutional Guidelines for Animal Care. The animal experiment protocol was approved by the Ethics Committee of the Second Affiliated Hospital of Zhejiang University School of Medicine [Approval No.: 006 (2021)].

Ubiquitylation assay

The HEK 293 cells were transfected with the indicated constructs, including Flag-MCL1, BEX2-MYC, K48R, FBXW7, and BTRC, for 24 h, preceded by a 15 μM MG132 (MCE) pre-treatment for 8 h. The BEX2-NC-HCT116 and BEX2-OE-HCT116 cells were transfected with the indicated constructs and also pre-treated with 15 μM MG132 (MCE) for 8 h. Proteins from whole-cell lysates were subsequently extracted, sonicated, and diluted 10 times with NP-40 lysis buffer, then supplemented with protease inhibitor cocktail (MCE) and immunoprecipitated with Flag beads. The ubiquitinated form of MCL1 was detected by western blot using anti-Ub antibody (Cell Signaling Technology, Beverly, MA, USA).

Co-immunoprecipitation (Co-IP) and immunoblotting (IB)

Cells were lysed using RIPA buffer [50 mM Tris-HCl (pH 7.5), 1% NP40, 0.35% DOC, 150 mM NaCl, 1 mM EDTA, and 1 mM EGTA supplemented with protease and phosphatase inhibitor cocktail; (MCE, Shanghai, China)] or IP lysis buffer [10 mM Tris-HCl (pH 7.5), 2 mM EDTA, 0.5% NP40, and 150 mM NaCl supplemented with protease and phosphatase inhibitor cocktail; (MCE, Shanghai, China)]. The cell lysates were centrifuged at 20,000 × *g* and 4°C for 10 min. The supernatants were then incubated with prepared bead-antibody complexes [10 μg of antibody and 50 μL of protein A/G magnetic beads; (Selleck, Shanghai, China)] or 5 μL of antibodies against Flag M2 magnetic beads (Sigma-Aldrich) at 4°C overnight. The proteins were electrophoresed in 12% SDS-PAGE, transferred to a PVDF membrane (Bio-Rad, Hercules, CA, USA), then incubated with a primary antibody at 4°C overnight and an appropriate secondary antibody for 1 h at room temperature (RT). The protein signal was visualized using an enhanced chemiluminescence substrate (YEASEN, Shanghai, China) and scanned using the Tanon 5200 chemiluminescence imaging system. The primary antibodies included rabbit anti-BEX2 (Sigma-Aldrich), rabbit anti-Flag (Cell Signaling Technology, Beverly, MA, USA), rabbit anti-MCL1 (Cell Signaling Technology), mouse anti-MYC (Cell Signaling Technology), mouse anti-Ub (Cell Signaling Technology), rabbit anti-NANOG (Proteintech, Rosemont, USA), rabbit anti-OCT4 (Proteintech), mouse anti-β-actin (Huabio), mouse anti-Lamin B1 (Proteintech), and rabbit anti-GAPDH (Proteintech).

Immunofluorescence analysis

Cells on coverslips were washed twice in PBS and permeabilized with 4% (w/v) paraformaldehyde (PFA) for 10 min at RT. The cells were permeabilized with 0.5% Triton X-100 (Sigma-Aldrich, St. Louis, MO, USA) in PBS for 15 min. Next, the cells were blocked with 1% bovine serum albumin [BSA] (Sigma-Aldrich, St. Louis, MO, USA) for 1 h, followed by incubation with anti-HA (Cell Signaling Technology) and anti-MCL1 antibodies (Cell Signaling Technology) at RT for 2 h. The cells were then incubated with Alexa Fluor 488- or Alexa Fluor 555-conjugated secondary antibodies (1:500; Abcam, Shanghai, China) for 1 h at RT. Nuclei were stained with DAPI for 5 min at RT, then observed under a Zeiss LSM 710 laser-scanning confocal imaging system (Carl Zeiss, Germany).

Quantitative real-time PCR (qRT-PCR)

Total RNA was extracted using TRIzol® reagent (Invitrogen) and cDNA was reversed-transcribed using the PrimeScript™

RT Master Mix (Takara, Beijing, China). Quantitative PCR was performed using the SYBR® Premix Ex Taq™ GC (Takara). GAPDH mRNA was used to normalize RNA inputs. The primers used for real-time PCR in the current study are listed in **Table S2**.

Transwell migration and Matrigel invasion assays

Cell migration was determined using the Transwell migration assay (8.0 μm pore size; Corning, NY, USA). DLD1 (2×10^4 and 4×10^4) or HCT116 cells (3×10^4 and 6×10^4) were seeded in serum-free medium in the upper chamber with or without Matrigel and the lower chamber was filled with RPMI-1640 medium containing 20% FBS. Non-migrating cells were removed after 36 h with cotton buds and the migrated cells were fixed with methanol, stained with crystal violet dye, and counted in nine different fields.

Wound healing assay

Cells were seeded in 6-well plates (Corning, NY, USA) for 24 h before being scratched with a 200-μL pipette tip. Wound healing within the same scraped line was examined and photographed at the indicated time points (0, 24, and 48 h) after rinsing the cells with PBS to remove cellular debris. Each experiment was repeated three times.

Cell viability assay

Cell viability was assessed using the Cell Counting Kit-8 [CCK-8] (Dojindo, Kumamoto, Jappan) following the manufacturer's protocol. Briefly, 5,000–7,000 cells per well were seeded in 96-well plates (Corning, NY, USA) and cultured for the specified duration. Subsequently, CCK-8 solution was added and the absorbance at 450 nm was determined using a SpectraMax microtiter plate reader (Molecular Devices, USA).

Gene set enrichment analysis (GSEA)

GSEA was performed on two groups (BEX2-WT and BEX2 KO) using the GSE112590 dataset to identify the most enriched and depleted KEGG pathways from the differentially expressed genes[20]. Differential genes between the high and low expression groups were subjected to enrichment analysis (FDR < 0.25 indicates statistical significance). The top 10 significantly enriched pathways were selected for further visual analysis.

Flow cytometric sorting

Cells were fully digested using trypsin (Gibco) and resuspended using 2% cell staining buffer (Biolegend, Shanghai, China), then labeled with APC-conjugated CD133 antibody (Biolegend). Flow cytometric sorting (BD FACSAria™ III, BD, SJ, CA, USA) was utilized using the BD FACSAria™ III to isolate specific DLD1 cells based on CD133 expression.

Extreme limiting dilution assay (ELDA)

Cells with reduced cell density were cultured in ultra-low adherence 96-well plates with fresh medium added every 3 d. The number of positive wells with spheroids was counted after 2 weeks of cell culture. Limiting dilution analysis was performed (http://bioinf.wehi.edu.au/software/elda/).

Nuclear and cytoplasmic protein extraction

Nuclear and cytoplasmic proteins were obtained using the Nuclear and Cytoplasmic Protein Extraction Kit (P0028; Beyotime, Shanghai, China) following the manufacturer's instructions.

Statistical analysis

All data were statistically analyzed using GraphPad Prism 6.0 (GraphPad Software, Inc., San Diego, CA, USA) and SPSS 20.0 (SPSS Inc, Chicago, IL, USA). A two-tailed t-test was utilized to compare the differences between the two groups. Pearson's test was used to determine correlations between clinicopathologic parameters and protein expression. Data are presented as the mean ± standard deviation (SD) or standard error of the mean (SEM). Statistical significance was set at a $P < 0.05$.

Results

Correlation of BEX2 expression with stemness markers and clinical characteristics of CRC

TCGA analysis revealed significantly reduced BEX2 expression in CRC tissues (**Figure 1A**). Kaplan-Meier analysis in GSE24551 indicated shortened disease-free survival (DFS) in the BEX2 low-expression group ($P = 0.02211$; **Figure 1B**). Meta-analysis across GEO datasets (GSE14333, GSE24549, and GSE24551) consistently demonstrated a direct correlation between higher BEX2 expression and improved disease-free

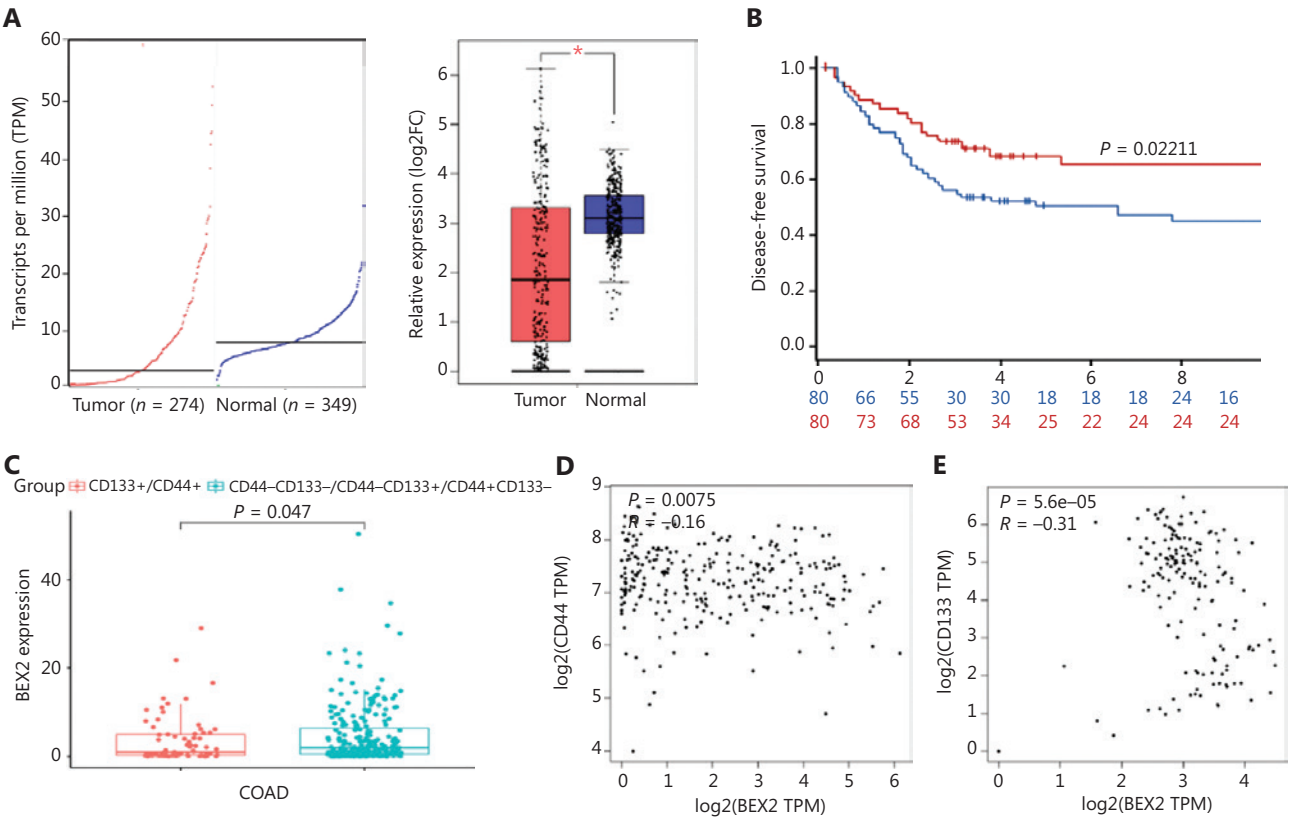


Figure 1 BEX2 downregulation in CRC is associated with poor prognosis and inversely correlates with stemness markers. (A) Comparison of BEX2 expression levels between colorectal tumor tissues (n = 274) and matched adjacent normal tissues (n = 349) based on data from TCGA. Expression values are presented as TPM. Statistical significance was assessed using the Wilcoxon signed-rank test. (B) The BEX2 low-expression group has a shorter DFS than the high-expression group in the GSE24551 database. Red represents the BEX2 high-expression group. Blue represents the BEX2 low-expression group, P = 0.02211. (C) The difference in the level of BEX2 expression in the two populations with strong stemness characteristics (CD133highCD44high) and weak stemness characteristics (CD133highCD44low, CD133lowCD44high, and CD133lowCD44low) in the TCGA database. (D, E) The correlation between BEX2 and stemness-related transcription factors (CD44 and CD133) in the TCGA and GTEx databases. COAD, colon adenocarcinoma; CRC, colorectal cancer; DFS, disease-free survival; TCGA, The Cancer Genome Atlas; TPM, transcripts per million.

survival (DFS) in CRC patients (**Figure S1**). Notably, BEX2 expression had a negative association with stemness markers (CD133 and CD44; **Figure 1C**). Molecular analysis using TCGA and GTEx databases indicated that BEX2 overexpression was associated with reduced CD44 and PROM1 (CD133) expression (**Figure 1D, E**). Therefore, there was a negative correlation between BEX2 and the stemness phenotype in CRC.

BEX2 knockout enhances CSC phenotypes in CRC *in vitro* and *in vivo*

BEX2-knockout cell lines were established in DLD1 cells (DLD1 KO and BEX2-KO-DLD1) and BEX2-overexpressing cell lines in HCT116 cells (HCT116 OE and BEX2-OE-HCT116) to further verify the relationship between BEX2 expression and stemness potential in CRC cells. Sphere-forming assays showed increased spheroid tumor proliferation in BEX2-KO-DLD1 cells and reduced proliferation in BEX2-OE-HCT116 cells (**Figure 2A, B**). Flow cytometry analysis revealed a higher proportion of CD133+ cells in the BEX2-knockout group compared to the control group (**Figure 2C, D**). CD133-positive cell populations in BEX2-OE-HCT116 cells showed significantly smaller and fewer spheres (**Figure S2A**). Pluripotency transcription factors (Nanog and OCT4) were more strongly expressed in CRC cells with low BEX2 levels (**Figures 2E, F and S2B**). BEX2-KO-DLD1 cells exhibited enhanced chemotherapy resistance to oxaliplatin (**Figure 2G**) and increased invasion and migration abilities (**Figure 2I, K**). In contrast, BEX2-OE-HCT116 cells exhibited a marked reduction in chemoresistance to oxaliplatin (**Figure 2H**) with significantly impaired invasive and migratory capabilities (**Figure 2J, L**). Rescue experiments confirmed that the observed effects were specifically due to BEX2

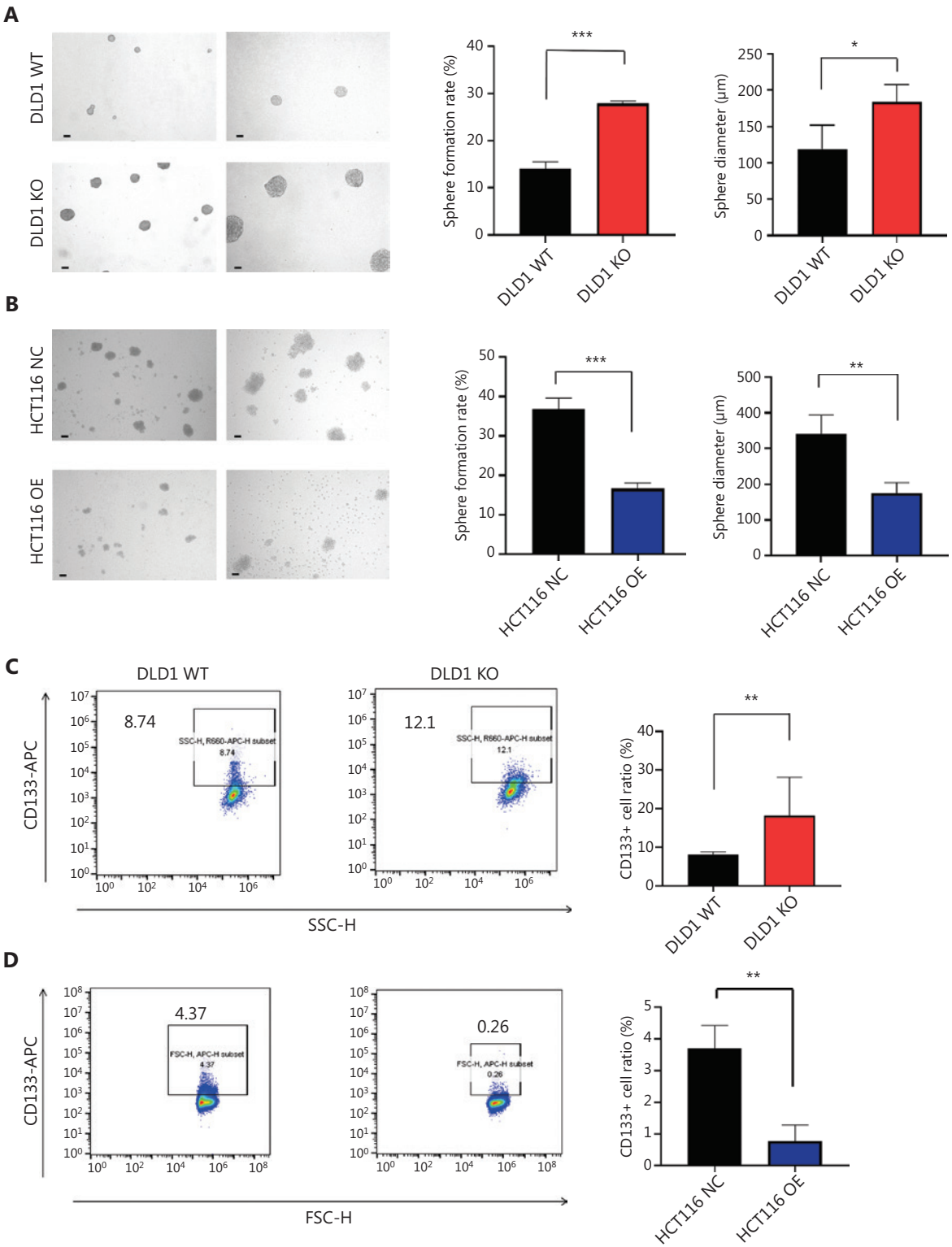


Figure 2 Continued

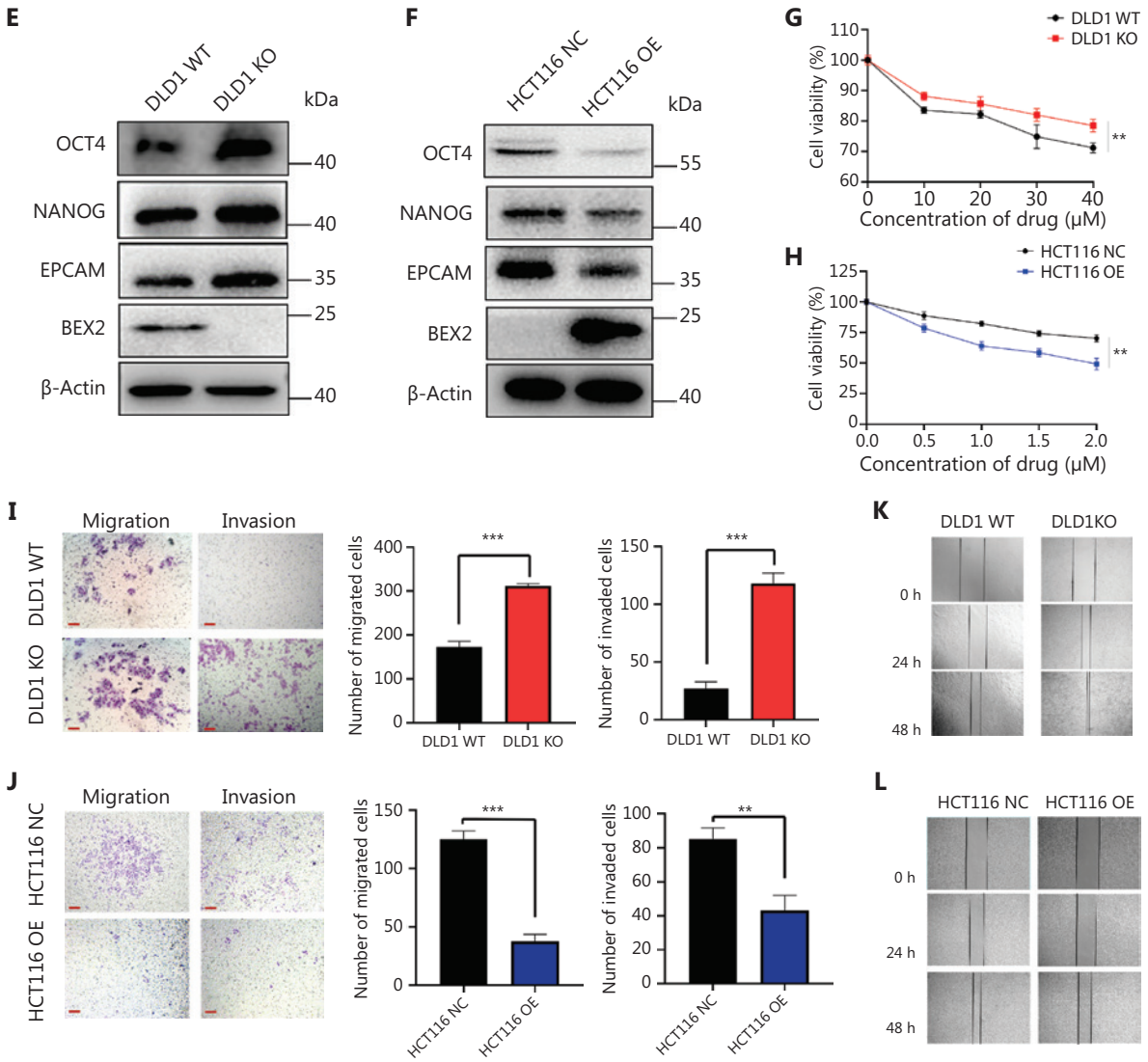


Figure 2 BEX2 expression influences the stemness characteristics of CRC. (A, B) Representative images of tumorspheres formed by BEX2 KO DLD1, BEX2 WT DLD1, BEX2 NC HCT116, and BEX2 OE HCT116 cells are shown. The graph shows the difference in the number of spheres at 100× or 200× magnification. Left: scale bar = 100 μm, Right: scale bar = 200 μm. The histogram shows the frequency and diameter of the cultured spheres. $^{**}P < 0.01$, $^{***}P < 0.001$, and $n = 3$ biologically independent samples per group. (C, D) FCM analyses of the CD133+ subpopulation percentage in CRC cells and $n = 3$ biologically independent samples per group. (E, F) Western blotting analysis was performed on OCT4, NANOG, and BEX2 expression in CRC cells. (G, H) Cell viability analysis of BEX2 KO DLD1, WT DLD1, BEX2 NC HCT116, and BEX2 OE HCT116 cells treated with 0–40 μM of Ox for 48 h. (I, J) Migration and invasion assays were performed. Experiments were repeated three times. Transwell assay detects the difference in cell migration ability at different levels of BEX2 expression. Scale bar = 200 μm. $^{*}P < 0.05$ and error bars represent the SD from three independent experiments. (K, L) A wound healing assay was performed to determine the effect of cell motility. CRC, colorectal cancer; FCM, flow cytometry; KO, knockout; NANOG, Nanog homeobox; NC, normal control; OCT4, octamer-binding transcription factor 4; OE, overexpression; Ox, oxaliplatin; SD, standard deviation; WT, wild type.

itself (**Figure S3**). ELDAs demonstrated that *BEX2* knockout cells had a stronger tumor presence compared to wild-type cells (**Figure S4A**). BEX2-OE-HCT116 cells were less tumorigenic than the control group (**Figure S4B**). *In vivo* studies showed that *BEX2* knockout significantly increased tumorigenicity with larger tumors formed from as few as 1×10^4 cells in the BEX2-KO-DLD1 group (**Figures 3A-D** and **S5A**). Conversely, the BEX2-OE-HCT116 group exhibited reduced tumorigenesis with the same cell count in NOD/SCID mice (**Figures 3E and S5C**). Tumorigenesis was noted in DLD1 cells with 1×10^2–1×10^5 cells and in HCT116 cells with 1×10^2–1×10^5 cells (**Figure S5A–D**). Collectively, these findings underscored that *BEX2* knockout enhances stem cell marker expression and spheroid growth under stem cell-permissive conditions in CRC cells.

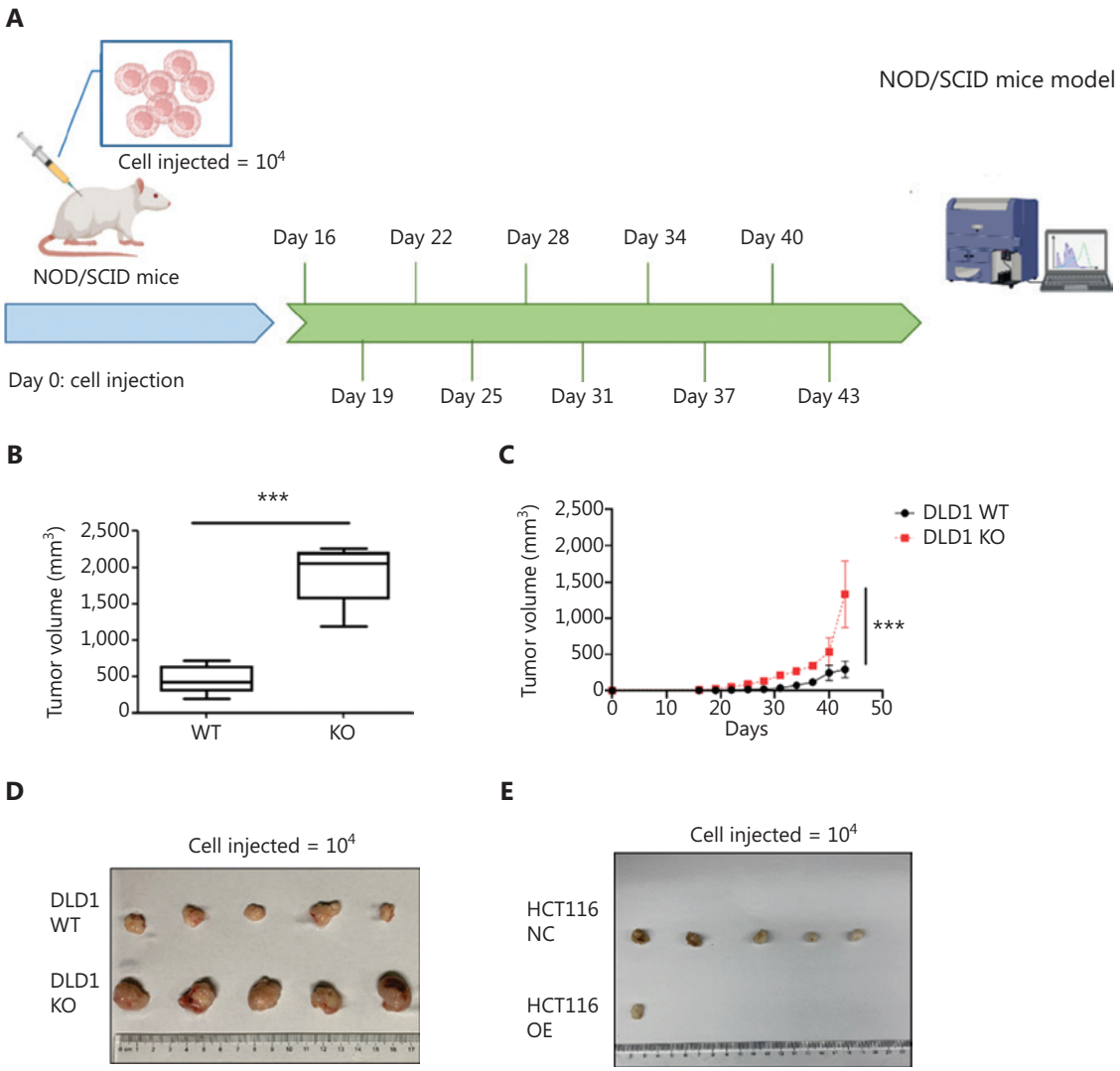


Figure 3 Low BEX2 expression promotes tumorigenesis in mice. CRC cells (10^2–10^5 cells per mouse) with BEX2 WT/KO or NC/OE were subcutaneously injected into NOD/SCID mice. Tumor formation ability and tumor characteristics were analyzed. (A) DLD1 cells with BEX2 WT/KO or HCT116 cells and BEX2 NC/OE were subcutaneously injected (1×10^4 cells per mouse) into 6-week-old female NOD/SCID mice. Tumor formation ability was analyzed. (B, C) Tumorigenicity experiments showed a difference in tumor volume between the BEX2 WT and the BEX2 KO groups *in vivo*. Tumor volumes were measured every 3 d (C), $n = 5$, ***$P < 0.001$, 2-way ANOVA. (D, E) Representative photographs of DLD1 with BEX2 WT/KO (D) [$n = 5$] or HCT116 with NC/OE (E) [$n = 6$] tumor formation in NOD/SCID mice. Each bar represents the mean ± SD. ***$P < 0.001$, 2-way ANOVA. CRC, colorectal cancer; KO, knockout; NC, normal control; OE, overexpression; WT, wild type.

BEX2 inhibits the potential of cancer stemness characterization by up-regulating the Hh signaling

Gene Set Enrichment Analysis [GSEA] (**Figure 4A**) was performed to explore the mechanistic intricacies of the BEX2 impact on CRC cell stemness characterization. The analysis was performed using CRC tissue data from GSE112590 with BEX2 expression subgroups defined by the median level of BEX2 expression as the cut-off. Pathways related to African trypanosomiasis, fat digestion and absorption, nitrogen metabolism, primary bile acid biosynthesis, and vitamin digestion and absorption were most significantly enriched, as shown in **Figure 4A**. The analysis highlighted a significant enrichment of the Hh signaling pathway in the BEX2 low-expression group (**Figure 4B**). Notably, Gli1, PTCH1, and HHIP (**Figure 4C**) were substantially upregulated in BEX2-KO-DLD1 cells compared to the control group, whereas BEX2-OE-HCT116 cells showed a significant decrease in these markers (**Figure 4D**). Western blot analysis corroborated the elevated expression of Gli1 and PTCH1

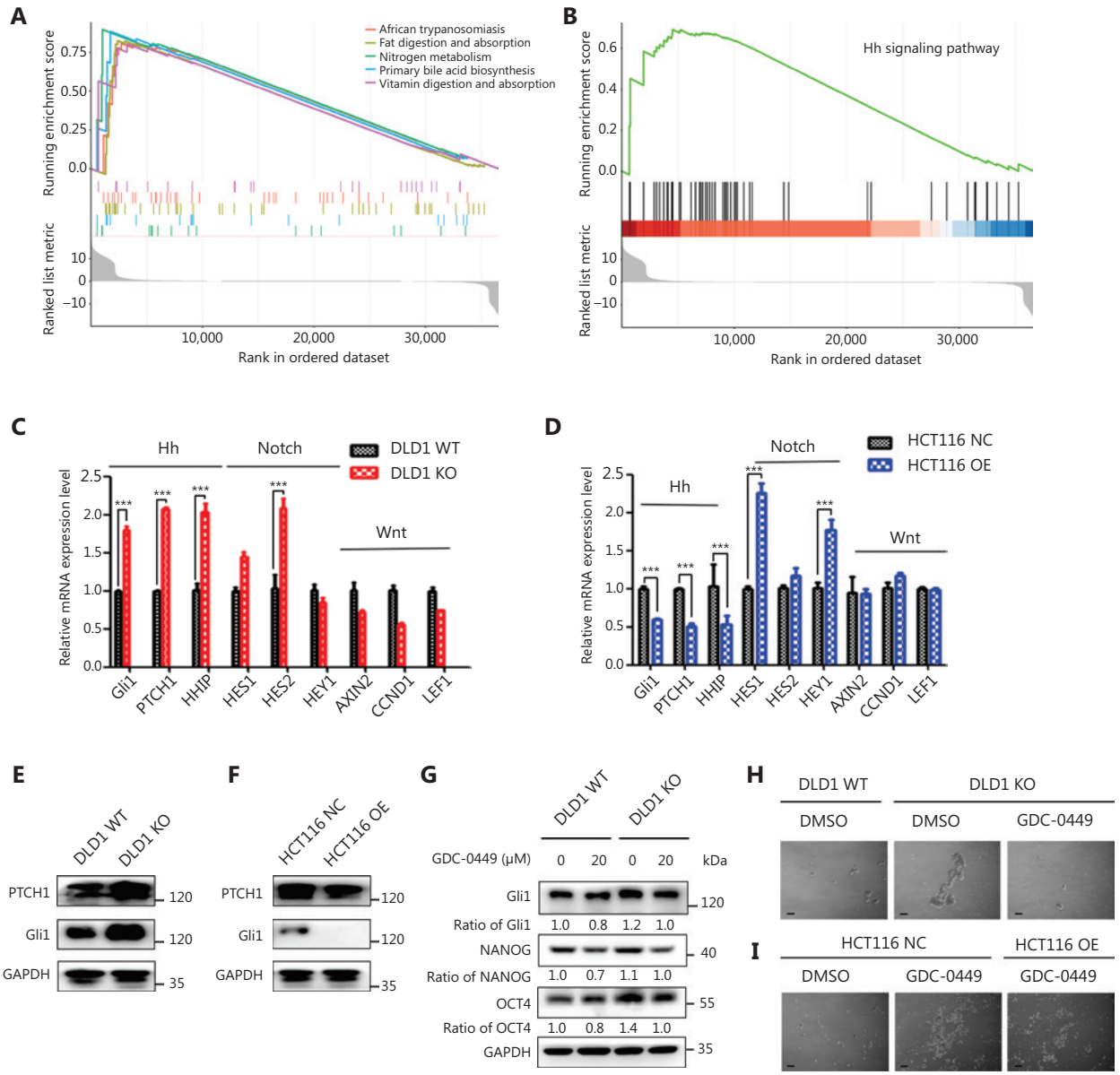


Figure 4 BEX2 inhibits tumor stemness by regulating the Hh signaling pathway. (A, B) GSEA results were obtained by analyzing the differential levels of BEX2 expression. (C, D) qRT-PCR analysis of the mRNA levels in the indicated CRC cell genes with or without knockout or overexpression of BEX2 and n = 3 biologically independent samples per group. (E, F) Immunoblotting analyses of DLD1 cells with or without *BEX2* knockout and HCT116 cells with or without BEX2 overexpression were performed with the antibodies, as indicated. GAPDH was used as the loading sample control. (G) BEX2 WT and BEX2 KO DLD1 cells were treated with or without 20 μM GDC-0449 for 8 h and immunoblotting analyses were performed. (H, I) DLD1 cells with or without *BEX2* knockout and HCT116 cells with or without BEX2 overexpression were treated with or without 10 μM GDC-0449 for 8 h and representative images of tumorspheres are shown. Spheres were cultured for 9 d before counting. The graph shows the difference in the number of spheres at 100× magnification. Scale bar = 100 μm. Each bar represents the mean ± SD. ***P < 0.001, 2-way ANOVA. CRC, colorectal cancer; GAPDH, glyceraldehyde-3-phosphate dehydrogenase; GSEA, gene set enrichment analysis; Hh, Hedgehog; KO, knockout; NC, normal control; OE, overexpression; SD, standard deviation; WT, wild type.

in BEX2-KO-DLD1 cells and the reduction in BEX2-OE-HCT116 cells (**Figure 4E, F**). Importantly, the Hh pathway inhibitor, GDC-0449, effectively reversed the effects induced by low BEX2 expression, substantiating the involvement of the Hh signaling pathway (**Figure 4G**). Treatment with GDC-0449 not only inhibited sphere formation in BEX2-KO-DLD1 and HCT116 cells (**Figures 4H, I and S6**) but also confirmed that BEX2 regulates the potential of CRC

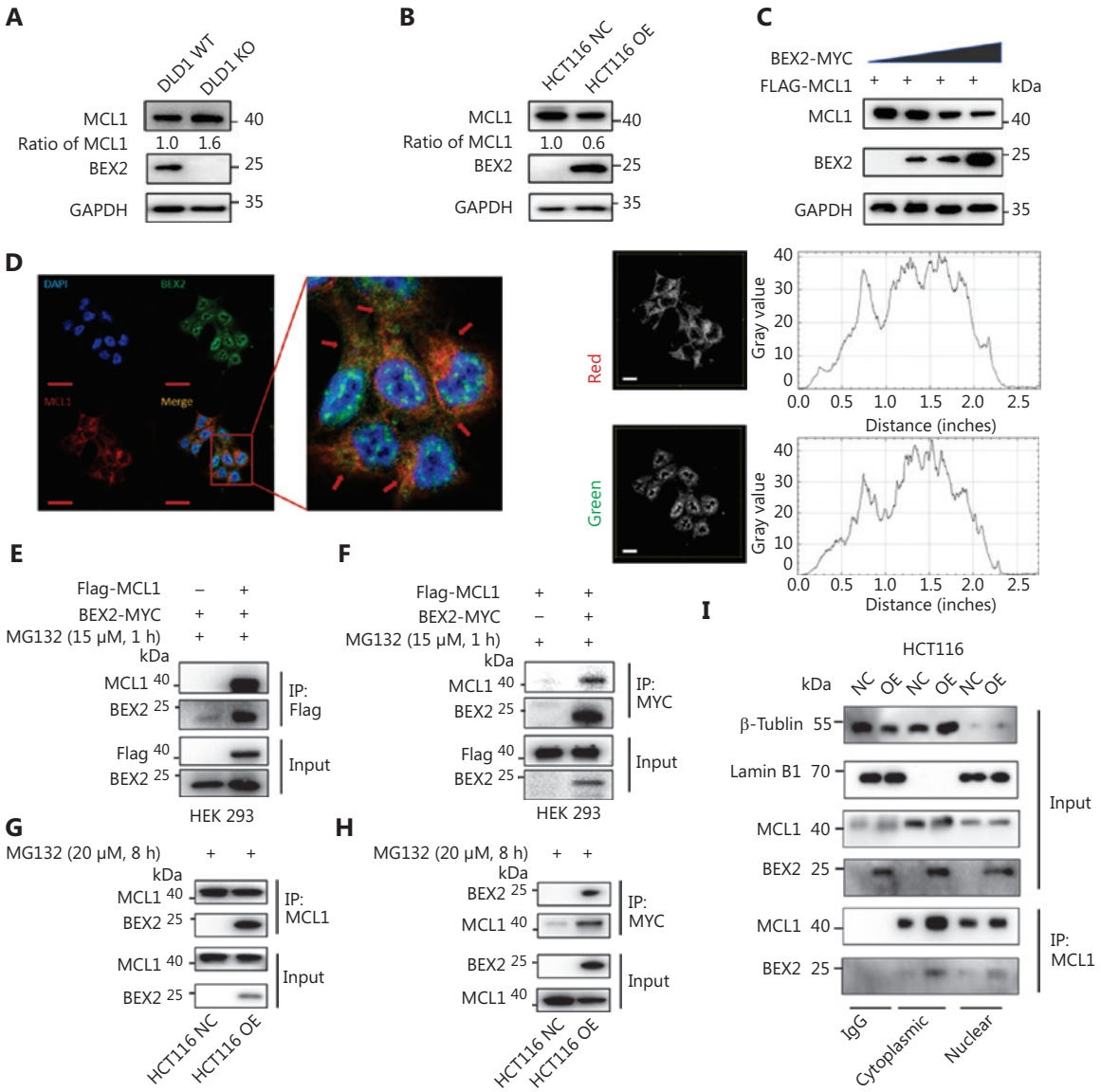


Figure 5 BEX2 interacts with MCL1 *in vitro* and *in vivo*. (A, B) Immunoblotting analyses of BEX2 KO DLD1, BEX2 WT DLD1, BEX2 NC HCT116, and BEX2 OE HCT116 cells were performed with the antibodies, as indicated. GAPDH was used as a loading sample control. (C) Western blotting analysis of MCL1 expression after HEK 293 cells were transfected with a mammalian expression vector encoding BEX2-MYC (0, 0.5, 1.0, and 2.0 μg) for 48 h. (D) Indirect immunofluorescence analysis of HCT116 cells with BEX2 and MCL1 antibodies was performed, counterstained with DAPI, then examined with a confocal microscope (scale bar = 40 μm). The right panel displays the Pearson's correlation coefficient quantifying the co-localization between BEX2 and MCL1 in immunofluorescence images. (E, F) HEK 293 cells were transfected with designated mammalian expression vectors encoding FLAG-MCL1 and BEX2-MYC or FLAG-MCL1 (E)/FLAG-MCL1 and BEX2-MYC or BEX2-MYC (F). After IP with anti-Flag (E) or anti-MYC (F) antibodies, BEX2 and MCL1 binding was analyzed by western blot. Before harvesting the cell lysate, the cells were treated with 15 μM MG132 for 1 h. (G, H) BEX2-NC-HCT116 and BEX2-OE-HCT116 were treated with MG132 (20 μM, 8 h). Whole cell lysate was treated with protein A/G beads pretreated with MCL1 antibody (G) and MYC magnetic beads (H). After IP with protein A/G beads and MYC magnetic beads, BEX2 and MCL1 binding was analyzed by western blot. (I) BEX2-NC-HCT116 and BEX2-OE-HCT116 were treated with nucleoplasmic separation reagent. The nuclear and cytoplasmic cell lysates were with protein A/G beads pretreated with MCL1 antibody. After IP with protein A/G beads, BEX2 and MCL1 binding was analyzed by western blot. DAPI, 4′,6-diamidino-2-phenylindole; IP, immunoprecipitation; KO, knockout; MCL1, myelogenous leukemia-1; NC, normal control; OE, overexpression; WT, wild type.

cell stemness characterization through an Hh signaling-dependent mechanism. These findings underscore the intricate interplay between BEX2 and the Hh signaling pathway in modulating the stemness properties of CRC cells.

BEX2 attenuates MCL1 stability *via* the ubiquitin-mediated proteasomal system

Previous studies have suggested interactions between BCL-2 family members and BEX2[21]. The crosstalk between BEX2 and MCL1 was explored given the established role of MCL1 in maintaining cancer stemness[15,16]. BEX2-KO-DLD1 cells showed elevated MCL1 expression compared to controls, while BEX2 overexpression in CRC cells led to reduced MCL1 levels that was confirmed by western blot (**Figure 5A, B**). Immunoblot analysis further substantiated a negative correlation between BEX2 and MCL1 expression (**Figure 5C**). Co-IP analysis confirmed the interaction between BEX2-MYC and FLAG-MCL1 co-expressed in HEK 293 cells (**Figure 5D, E**). Semi-endogenous BEX2 and endogenous MCL1 were co-precipitated in HCT116 cells under physiologic conditions (**Figure 5F, G**). In addition, co-localization of MCL1 and BEX2

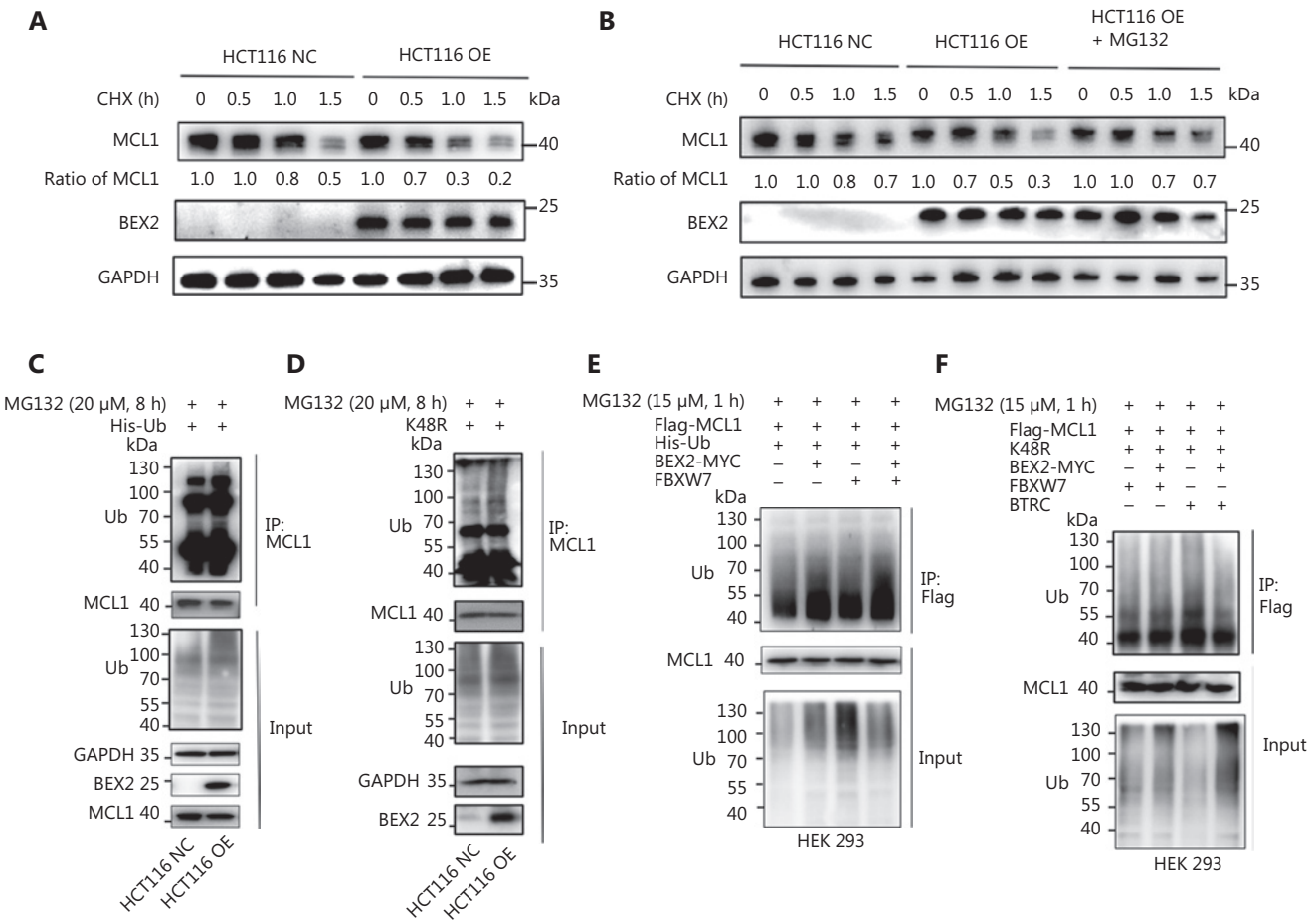


Figure 6 BEX2 attenuates MCL1 stability *via* the ubiquitin-proteasome system. (A) BEX2 NC HCT116 and BEX2 OE HCT116 cells were treated with CHX (100 μg/mL) for different periods. Quantitation was performed by densitometry with ImageJ software. (B) BEX2 NC HCT116 and BEX2 OE HCT116 cells were treated with CHX (100 μg/mL), followed by treatment with or without MG132 (20 μM, 8 h). Immunoblotting analyses were performed with antibodies against MCL1, BEX2, and GAPDH. MCL1 band intensities were normalized according to the GAPDH level and MCL1 in the CHX-untreated BEX2 NC HCT116 cells. (C, D) Endogenous ubiquitination of MCL1 in control and BEX2 overexpression of HCT116 cells that were assessed by immunoblot analysis with anti-ubiquitin after immunoprecipitation with anti-MCL1 (top) and immunoblot analysis with input proteins and loading controls (bottom). HCT116 NC and HCT116 OE were treated with MG132 (20 μM, 8 h). (E, F) HEK 293 cells expressing His-Ub or K48R were treated with MG132 (15 μM for 8 h). The lysate was subjected to pulldown with Flag beads. Ubiquitination of FLAG-MCL1 was analyzed when FBXW7 and BTRC were overexpressed. BTRC, beta-transducin repeat containing E3 ubiquitin protein ligase; CHX, cycloheximide; FBXW7, F-box and WD repeat domain containing 7; GAPDH, glyceraldehyde-3-phosphate dehydrogenase; MCL1, myelogenous leukemia-1; NC, normal control; OE, overexpression.

in the cytoplasm was demonstrated through immunofluorescence in HEK 293 cells (**Figure 5H**). Co-IP analysis was used to confirm the interaction between BEX2 and MCL1 in protein extracts from the cytoplasm and nucleus of HCT116 cells. The results demonstrated increased binding between BEX2 and MCL1 in the cytoplasm (**Figure 5I**). The results showed that BEX2 binds to MCL1 in the cytoplasm and nucleus.

The molecular mechanism by which BEX2 interacts with *MCL1* expression was subsequently probed. Surprisingly, the *MCL1* mRNA level showed no significant difference between BEX2-OE-HCT116 and control cells (**Figure S7A**). Notably, chloroquine (CQ) treatment did not alter MCL1 expression in HCT116 cells overexpressing BEX2 (**Figure S7B**), suggesting that BEX2-mediated MCL1 regulation operates independent of autophagy inhibition. Conversely, treatment with cycloheximide (CHX) resulted in a time-dependent decrease in MCL1 protein levels (**Figure 6A**), suggesting that BEX2 influences the stability of MCL1. A previous study showed that the ubiquitin-proteasome system may regulate the stability of MCL1[22], so whether BEX2 promotes MCL1 degradation in a proteasome-dependent manner was tested. Notably, the proteasome inhibitor, MG132, inhibited the degradation of endogenous MCL1 protein under conditions of BEX2 overexpression (**Figure 6B**), indicating that BEX2 may promote ubiquitin-proteasome-dependent degradation of MCL1. Further analysis revealed that BEX2 overexpression led to a typical ubiquitination smear in the presence of MG132, indicating enhanced polyubiquitination of MCL1 (**Figures 6C, D and S7C**). Considering that FBXW7 and BTRC are known E3 ligases implicated in the ubiquitination-mediated degradation of MCL1[23-25], FBXW7 plasmids were introduced and increased ubiquitination of MCL1 was noted (**Figure 6E, F**). Co-IP assays were performed in HEK 293 cells co-transfected with BEX2-MYC and Flag-BTRC or Flag-FBXW7. The results demonstrated the interaction between BEX2 and BTRC but not with FBXW7 (**Figure S7D, E**). These results collectively suggested that BEX2 promotes the ubiquitination of MCL1 through BTRC, leading to MCL1 degradation.

BEX2 inhibits the potential of CRC stemness characterization by facilitating ubiquitination of MCL1

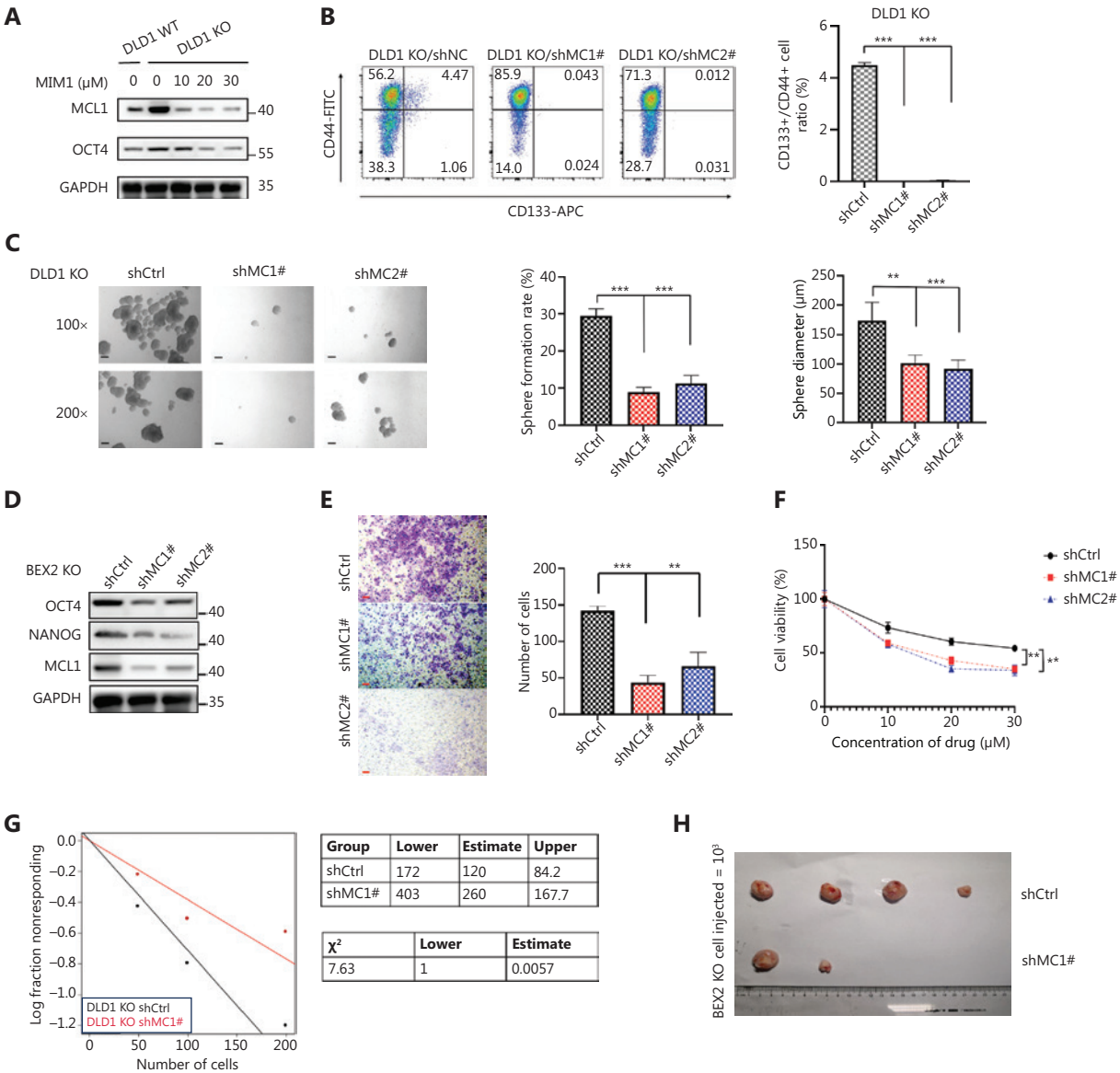
An MCL1-specific inhibitor (MIM1) was used in BEX2-KO-DLD1 cells to discern the impact on stemness-related genes and further elucidate the regulatory role of MCL1 in the potential of CRC cell stemness characterization orchestrated by BEX2. Treatment with MIM1 significantly suppressed the expression of key markers associated with CSCs in CRC cells (**Figures 7A** and **S8A**). By leveraging *MCL1* shRNA to silence *MCL1* in BEX2-KO-DLD1 cells, knockdown efficiency was subsequently confirmed through qRT-PCR and western blot analyses (**Figure S8B, C**). Suppression of MCL1 expression in BEX2-KO-DLD1 cells partially reversed the increase in the CD44+CD133+ cell population (**Figure 7B**). The formation of spheres in shMCL1-BEX2-KO-DLD1 cells was significantly diminished compared to the control group (**Figure 7C**) and accompanied by a substantial reduction in NANOG and OCT4 expression (**Figure 7D**). Flow cytometric sorting by CD133 revealed significantly reduced levels of OCT4 and NANOG in shMCL1-BEX2-KO-DLD1 cells compared to shCtrl-BEX2-KO-DLD1 cells (**Figure S8D**). Notably, the migratory and invasive capabilities of shMCL1-BEX2-KO-DLD1 cells were attenuated compared to the control group (**Figures 7E and S8E**). Moreover, shMCL1-BEX2-KO-DLD1 cells exhibited heightened sensitivity to chemotherapy (**Figure 7F**). In addition, knockdown of *MCL1* expression in BEX2-KO-DLD1 cells partially mitigated the enhanced sphere formation capability observed in ELDAs, as shown in **Figure 7G**. Mice were injected with DLD1 cells and BEX2 depletion in the presence or absence of *MCL1* shRNA expression to further examine the role of BEX2 impacting the MCL1-Hh signaling axis in regulating the potential of CRC cell stemness. Depletion of BEX2 enhanced tumor growth, which was counteracted by the expression of *MCL1* shRNA (**Figures 7H and S8F**). These findings suggested that BEX2 reduces CRC cell stemness by promoting MCL1 ubiquitination and degradation.

Discussion

CRC remains a major health threat due to high rates of metastasis, recurrence, and resistance to treatment, all of which contribute to poor patient outcomes[26]. The CSCs within CRC are known for heightened resistance to treatments and greater metastatic potential[27-29]. These CSCs are critically involved in the recurrence of CRC following conventional therapies[30,31]. Notably, chemotherapy can increase the number of CSCs in CRC tissues, highlighting the clinical importance[32]. Understanding the molecular mechanisms that regulate and maintain CSCs in CRC is crucial for developing effective therapeutic strategies.

Recent studies have underscored the heterogeneity of CRC CSCs with respect to phenotype, function, and transcriptomics[33]. Markers, such as CD44[34] and CD133[35], are widely used to identify and characterize these CSCs, which helps in understanding the diverse nature of these cells. Exploring the genes and regulatory mechanisms affecting CSCs in CRC could significantly advance clinical treatment approaches.

The current study revealed that *BEX2*, a gene associated with malignant characteristics in CRC[19,36], has a critical role in regulating the stemness potential of CRC. Reduced *BEX2* expression was shown to be correlated with heightened stemness features and poorer prognosis in CRC patients. Specifically, BEX2 was shown to facilitate degradation of MCL1 and inhibit Hh signaling, thereby diminishing the stemness potential of CRC cells. MCL1, a member of the BCL-2 anti-apoptotic family, is crucial for cancer cell survival by resisting apoptosis.



Group	Lower	Estimate	Upper
shCtrl	172	120	84.2
shMC1#	403	260	167.7

X^2	Lower	Estimate
7.63	1	0.0057

Figure 7 BEX2 inhibits cancer stemness through MCL1 in CRC. (A) The MCL1-specific inhibitor, MIM1 (10 and 20 μM), was used in DLD1 cell lines (BEX2 WT and BEX2 KO). The protein was extracted after 16 h and stemness marker expression was detected by western blot. (B–H) Stable cell lines were screened with puromycin (5 μg/mL) and the assays were performed after 48 h of infection of BEX2 KO DLD1 cells with non-targeting control shRNA or *MCL1* shRNA: (B) FCM analysis of CD44+CD133+ expression in cells and n = 3 biologically independent samples per group. (C) Determination of cell sphere formation. The graph shows the difference in the number of spheres at 100× or 200× magnification. Scale bar = 400 or 200 μm. Mean ± standard deviation (n = 3); $^{**}P < 0.01$, $^{***}P < 0.001$. (D) Western blot analysis of NANOG and OCT4 expression in DLD1 cells with or without depletion of MCL1 in the presence of *BEX2* knockout. (E) Migration assays. Mean ± standard deviation (n = 3); $^{**}P < 0.01$, $^{**}P < 0.001$. (F) Apoptosis induced by Ox (48 h). Mean ± standard deviation (n = 3). $^{*}P < 0.05$. (G) Tumorigenic cell frequency of shCtrl and shMC1# spheroid cells was determined with ELDA assays (http://bioinf.wehi.edu.au/software/elda/). (H) *In vivo* tumorigenicity experiment (5 × 10^3 cells/site, 6 weeks, n = 6). Representative photographs of DLD1 BEX2 KO with shCtrl or shMCL1-1# tumor formation in NOD/SCID mice. CRC, colorectal cancer; Ctrl, control; ELDAs, extreme limiting dilution assays; FCM, flow cytometry; KO, knockout; sMCL1, myelogenous leukemia-1; NANOG, Nanog homeobox; OCT4, octamer-binding transcription factor 4; Ox, oxaliplatin.

MCL1 is frequently amplified and overexpressed in various cancers, particularly in patients with chemotherapy-resistant tumors. For example, *MCL1* gene amplification is prevalent in drug-resistant triple-negative breast cancer (TNBC) after neoadjuvant chemotherapy[37] and elevated MCL1 levels have been reported in chemotherapy-resistant ovarian cancer patients[14].

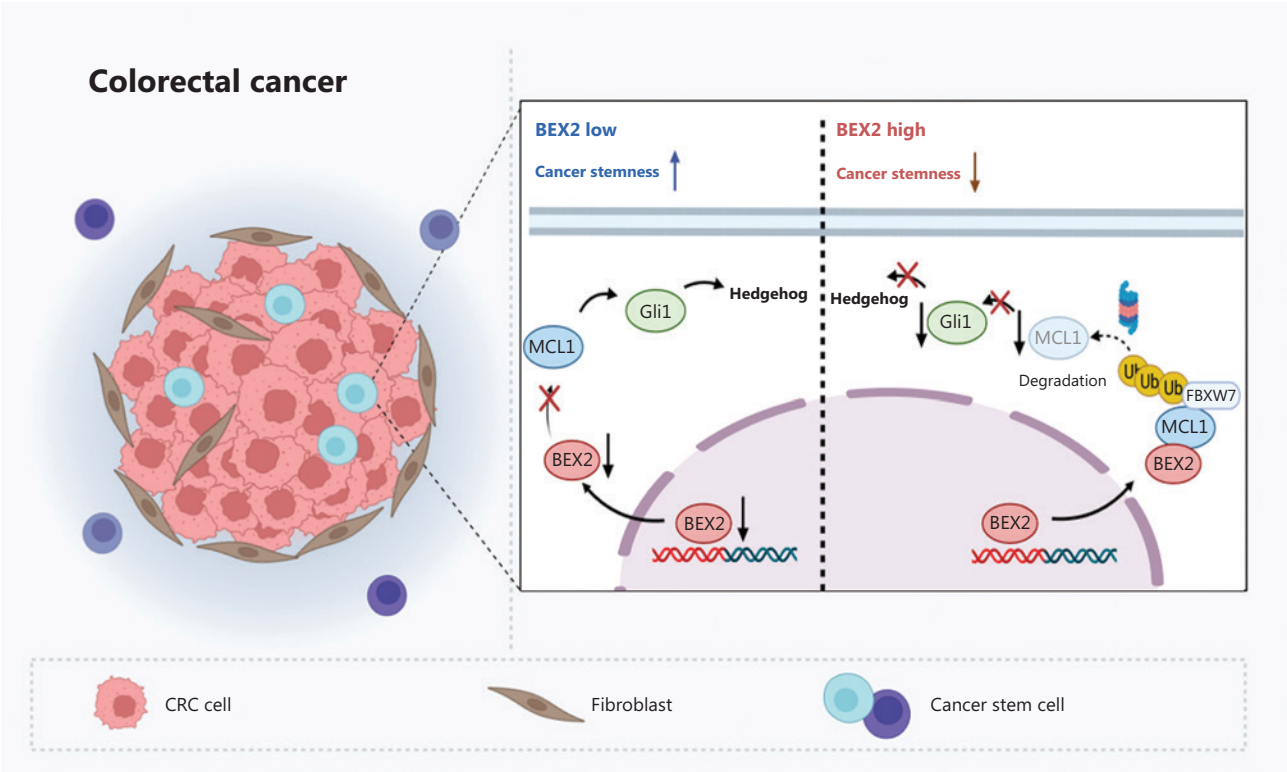


Figure 8 Working model: Cancer stemness regulation by BEX2 in colorectal cancer. BEX2 binds to MCL1 and facilitates FBXW7-mediated ubiquitination and degradation of MCL1 in CRC cells with high BEX2 expression. This process suppresses the Hedgehog signaling pathway, thereby inhibiting cancer stemness. Conversely, in CRC cells with low BEX2 expression, reduced BEX2-MCL1 binding diminishes MCL1 ubiquitination and degradation. Consequently, elevated MCL1 expression attenuates suppression of the Hedgehog signaling pathway, enhancing cancer stemness and promoting malignant progression of CRC. CRC, colorectal cancer; FBXW7, F-box and WD repeat domain containing 7; MCL1, myelogenous leukemia-1.

The current study highlighted the importance of MCL1 in the stemness regulation mechanism mediated by the BEX2-MCL1-Hh signaling pathway. MCL1 modulates the expression of stemness-related proteins, chemoresistance, invasive potential, and tumorigenicity in CRC cells.

Interestingly, MCL1 interacts with the Hh inhibitory factor, SUFU, disrupting the inhibitory effect on Gli1 and activating the Hh pathway[12]. Co-IP confirmed direct binding between MCL1 and Gli1, as evidenced by immunoprecipitation of MCL1 followed by Gli1 immunoblotting (**Figure S9**). The Hh, Wnt/β-catenin, and Notch signaling pathways are known to significantly impact tumor cell stemness characteristics[38-40]. The current study adds to this knowledge by demonstrating that BEX2 inhibits Hh signaling by facilitating MCL1 degradation. This finding suggests a mechanism in which BEX2 negatively regulates Hh signaling to attenuate CRC stemness.

Furthermore, alterations in the CD133+CD44+ and CD44+CD133− cell subsets, were noted, suggesting a complex interplay between MCL1 and CRC CSC markers. Inhibition of MCL1 may selectively affect CD133+CD44+ CSCs, promoting quiescence or differentiation while enhancing the proliferation of the CD44+CD133− subpopulation. This finding highlights the multifaceted role of MCL1 in regulating CRC stemness and the need for further research to fully elucidate its therapeutic implications.

The suppression of BEX2 in specific CRC subtypes, particularly those with mesenchymal or stem-like phenotypes, likely reflects convergent regulatory mechanisms at multiple levels, including epigenetic silencing, transcriptional repression, and post-transcriptional control[41]. Emerging evidence indicates that DNA hypermethylation of promoter CpG islands is a hallmark of CRCs exhibiting the CpG island methylator phenotype (CIMP), leading to silencing of tumor-suppressive genes early in tumorigenesis. For example, promoter methylation of PRMT5[42] and PTGER4[43] has been proposed as diagnostic biomarkers in CIMP-positive CRCs, underscoring the role of DNA methylation in subtype-specific gene downregulation[44]. By analogy, hypermethylation of the BEX2 promoter could account for the diminished expression in stemness-prone CRC subgroups, thereby stabilizing MCL1 and promoting Hh

pathway activation. In addition, transcriptional repression by oncogenic factors, such as FOXA1, which modulates chromatin accessibility in metastasis-associated gene networks[45], may further curtail *BEX2* expression in aggressive CRC subtypes. Finally, post-transcriptional regulation *via* miRNA networks could contribute to *BEX2* mRNA degradation, as has been documented for analogous stemness-associated genes in CRC[46,47].

Abnormal activation of the Hh signaling pathway in CSCs is a critical driver of CRC treatment resistance[48,49]. Targeting molecules involved in this pathway holds promise for reversing resistance in adenocarcinoma therapy[4]. In the initial study, *BEX2* knockout enhanced CRC cell migration and metastasis *via* nuclear translocation of Zic2, which activated the Hh signaling pathway[19]. The findings herein indicated that BEX2, by inhibiting the Hh signaling pathway, reduces the stemness potential of CRC cells (**Figure 8**). In additon, targeting MCL1 could provide a novel approach to overcome drug resistance in CRC. The apparent paradox of BEX2 dual roles is reconciled by partitioned interactions, as follows: cytoplasmic sequestration of Zic2 to inhibit metastasis versus scaffolding MCL1 for degradation to suppress stemness, reflecting stage- and context-dependent substrate availability and signaling priorities. Consequently, therapeutic strategies aimed at restoring BEX2 function or mimicking its interactions could simultaneously block metastatic spread and eradicate cancer stem cells, offering a multifaceted approach to improve CRC patient outcomes. This effect is attributable not only to the MCL1' interaction with the Hh signaling pathway but also to the critical role in altering the metabolic state of tumor cells and regulating stemness through mitochondrial respiration[15].

In summary, the current study elucidates the regulatory network involving BEX2, MCL1, and the Hh signaling pathway in modulating CRC stemness characteristics. BEX2 was shown to regulate Hh signaling and MCL1, contributing to a reduction in CRC cell stemness potential. This regulatory mechanism appears to function independently of the Wnt and Notch signaling pathways. In addition, inhibiting *MCL1* genetically or pharmacologically diminishes stemness potential and enhances chemotherapy efficacy. These findings highlight the potential of BEX2 and MCL1 as novel therapeutic targets, particularly for drug-resistant CRC cases characterized by MCL1 amplification. While the current findings underscore the therapeutic potential of targeting the BEX2-MCL1-Hh axis in CRC, several limitations warrant consideration. First, the mechanisms underlying BEX2 suppression in specific CRC subtypes have not been completely elucidated. Further validation is required to confirm whether BEX2 downregulation in stemness-prone subtypes arises from epigenetic modifications or transcriptional repression by oncogenic regulators. Second, clinical translation of MCL1 inhibitors faces challenges, including on-target toxicity in normal tissues and compensatory activation of alternative anti-apoptotic pathways. Third, while BEX2 exhibit stemness-suppressive properties, BEX2 overexpression promotes invasion and migration. Finally, the interplay between BEX2 and other stemness-related pathways, such as Wnt/β-catenin or Hippo signaling, remains unexplored, necessitating multi-omics approaches to delineate context-dependent crosstalk. Addressing these limitations will refine subtype-specific therapeutic strategies and enhance the clinical feasibility of targeting this axis.

Conclusions

Overall, the current study demonstrated that BEX2 functions as a key negative regulator of stemness characteristics in CRC cells. The findings revealed that BEX2 interacts with MCL1 and promotes ubiquitin-mediated degradation *via* the proteasomal pathway. This degradation of MCL1 subsequently leads to inhibition of the Hh signaling pathway, ultimately suppressing cancer stemness properties, such as tumor sphere formation, expression of stemness markers, chemoresistance, and invasive capabilities. Use of the Hh pathway inhibitor, GDC-0449, or knockdown of MCL1 effectively reversed the stemness-enhancing effects induced by BEX2 deficiency. These findings not only elucidate a novel molecular mechanism by which BEX2 modulates CRC stemness but also suggest that BEX2 could serve as a potential prognostic biomarker. Targeting the BEX2-MCL1 axis may offer a promising strategy for developing new therapeutic interventions against CRC.

Acknowledgments

We acknowledge the generous support of the Department of Colorectal Surgery and Oncology, Key Laboratory of Cancer Prevention and Intervention, Ministry of Education, The Second Affiliated Hospital, Zhejiang University School of Medicine. We are grateful to all the participants who have made this research possible.

Grant support

This research was supported by the National Natural Science Foundation (Grant No. 81802750, 82072624, and 82102708), Fundamental Research Funds for the Central Universities (Grant No. 226-2024-00176), Zhejiang Provincial Natural Science Foundation of China (Grant No. LMS25H160014), and Zhejiang Provincial Medicine and Technology Projects Grant (Grant No. 2020RC063).

Conflict of interest statement

No potential conflicts of interest are disclosed.

Author contributions

Conceived and designed the analysis: Yeting Hu, Kefeng Ding.
Collected the data: Yucheng Qian, Jingsun Wei, Yuan Bian, Yimin Fang, Xiaoxu Ge.
Contributed data or analysis tools: Yinuo Tan, Liubo Chen, Kai Jiang, Dongliang Fu, Qian Xiao.
Performed the analysis: Yucheng Qian, Jingsun Wei, Yuan Bian, Tianyi Ling.
Wrote the paper: Yucheng Qian.

Data availability statement

The data generated in this study are available upon request from the corresponding author.

References

1. Kriplani P, Guarve K. Nanotechnology a boon for colorectal cancer treatment. Recent Pat Anticancer Drug Discov. 2023; 18: 379-96.
2. Siegel RL, Giaquinto AN, Jemal A. Cancer statistics, 2024. CA Cancer J Clin. 2024; 74: 12-49.
3. Ohta Y, Fujii M, Takahashi S, Takano A, Nanki K, Matano M, et al. Cell-matrix interface regulates dormancy in human colon cancer stem cells. Nature. 2022; 608: 784-94.
4. Xing P, Wang S, Cao Y, Liu B, Zheng F, Guo W, et al. Treatment strategies and drug resistance mechanisms in adenocarcinoma of different organs. Drug Resist Updat. 2023; 71: 101002.
5. Shen S, Vagner S, Robert C. Persistent cancer cells: the deadly survivors. Cell. 2020; 183: 860-74.
6. Walcher L, Kistenmacher AK, Suo H, Kitte R, Dluczek S, Strauss A, et al. Cancer stem cells-origins and biomarkers: perspectives for targeted personalized therapies. Front Immunol. 2020; 11: 1280.
7. Takahashi K, Tanabe K, Ohnuki M, Narita M, Ichisaka T, Tomoda K, et al. Induction of pluripotent stem cells from adult human fibroblasts by defined factors. Cell. 2007; 131: 861-72.
8. Jeter CR, Liu B, Liu X, Chen X, Liu C, Calhoun-Davis T, et al. NANOG promotes cancer stem cell characteristics and prostate cancer resistance to androgen deprivation. Oncogene. 2011; 30: 3833-45.
9. Prasetyanti PR, Medema JP. Intra-tumor heterogeneity from a cancer stem cell perspective. Mol Cancer. 2017; 16: 41.
10. Takebe N, Miele L, Harris PJ, Jeong W, Bando H, Kahn M, et al. Targeting Notch, Hedgehog, and Wnt pathways in cancer stem cells: clinical update. Nat Rev Clin Oncol. 2015; 12: 445-64.
11. Wicking C, Smyth I, Bale A. The Hedgehog signalling pathway in tumorigenesis and development. Oncogene. 1999; 18: 7844-51.
12. Wu X, Zhang LS, Toombs J, Kuo YC, Piazza JT, Tuladhar R, et al. Extra-mitochondrial prosurvival BCL-2 proteins regulate gene transcription by inhibiting the SUFU tumour suppressor. Nat Cell Biol. 2017; 19: 1226-36.
13. Veleta KA, Cleveland AH, Babcock BR, He YW, Hwang D, Sokolsky-Papkov M, et al. Antiapoptotic Bcl-2 family proteins BCL-xL and MCL-1 integrate neural progenitor survival and proliferation during postnatal cerebellar neurogenesis. Cell Death Differ. 2021; 28: 1579-92.
14. Wu X, Luo Q, Zhao P, Chang W, Wang Y, Shu T, et al. MGMT-activated DUB3 stabilizes MCL1 and drives chemoresistance in ovarian cancer. Proc Natl Acad Sci U S A. 2019; 116: 2961-6.
15. Lee KM, Giltnane JM, Balko JM, Schwarz LJ, Guerrero-Zotano AL, Hutchinson KE, et al. MYC and MCL1 cooperatively promote chemotherapy-resistant breast cancer stem cells via regulation of mitochondrial oxidative phosphorylation. Cell Metab. 2017; 26: 633-47.e7.
16. Huskey NE, Guo T, Evason KJ, Momcilovic O, Pardo D, Creasman KJ, et al. CDK1 inhibition targets the p53-NOXA-MCL1 axis, selectively kills embryonic stem cells, and prevents teratoma formation. Stem Cell Reports. 2015; 4: 374-89.
17. Fernandez EM, Diaz-Ceso MD, Vilar M. Brain expressed and X-linked (Bex) proteins are intrinsically disordered proteins (IDPs) and form new signaling hubs. PLoS One. 2015; 10: e0117206.
18. Foltz G, Ryu GY, Yoon JG, Nelson T, Fahey J, Frakes A, et al. Genome-wide analysis of epigenetic silencing identifies BEX1 and BEX2 as candidate tumor suppressor genes in malignant glioma. Cancer Res. 2006; 66: 6665-74.
19. Tan Y, Hu Y, Xiao Q, Tang Y, Chen H, He J, et al. Silencing of brain-expressed X-linked 2 (BEX2) promotes colorectal cancer metastasis through the Hedgehog signaling pathway. Int J Biol Sci. 2020; 16: 228-38.
20. Subramanian A, Tamayo P, Mootha VK, Mukherjee S, Ebert BL, Gillette MA, et al. Gene set enrichment analysis: a knowledge-based approach for interpreting genome-wide expression profiles. Proc Natl Acad Sci U S A. 2005; 102: 15545-50.
21. Xiao Q, Hu Y, Liu Y, Wang Z, Geng H, Hu L, et al. BEX1 promotes imatinib-induced apoptosis by binding to and antagonizing BCL-2. PLoS One. 2014; 9: e91782.
22. Wu X, Luo Q, Liu Z. Ubiquitination and deubiquitination of MCL1 in cancer: deciphering chemoresistance mechanisms and providing potential therapeutic options. Cell Death Dis. 2020; 11: 556.
23. Ren H, Koo J, Guan B, Yue P, Deng X, Chen M, et al. The E3 ubiquitin ligases β-TrCP and FBXW7 cooperatively mediates GSK3-dependent Mcl-1 degradation induced by the Akt inhibitor API-1, resulting in apoptosis. Mol Cancer. 2013; 12: 146.
24. Inuzuka H, Shaik S, Onoyama I, Gao D, Tseng A, Maser RS, et al. SCF(FBW7) regulates cellular apoptosis by targeting MCL1 for ubiquitylation and destruction. Nature. 2011; 471: 104-9.
25. Yeh CH, Bellon M, Nicot C. FBXW7: a critical tumor suppressor of human cancers. Mol Cancer. 2018; 17: 115.
26. Colak S, Medema JP. Cancer stem cells – important players in tumor therapy resistance. FEBS J. 2014; 281: 4779-91.
27. Singh SK, Hawkins C, Clarke ID, Squire JA, Bayani J, Hide T, et al. Identification of human brain tumour initiating cells. Nature. 2004; 432: 396-401.

28. Lytle NK, Barber AG, Reya T. Stem cell fate in cancer growth, progression and therapy resistance. Nat Rev Cancer. 2018; 18: 669-80.
29. Cojoc M, Mabert K, Muders MH, Dubrovska A. A role for cancer stem cells in therapy resistance: cellular and molecular mechanisms. Semin Cancer Biol. 2015; 31: 16-27.
30. Colak S, Zimberlin CD, Fessler E, Hogdal L, Prasetyanti PR, Grandela CM, et al. Decreased mitochondrial priming determines chemoresistance of colon cancer stem cells. Cell Death Differ. 2014; 21: 1170-7.
31. Chen B, Zhang D, Kuai J, Cheng M, Fang X, Li G. Upregulation of miR-199a/b contributes to cisplatin resistance via Wnt/β-catenin-ABCG2 signaling pathway in ALDHA1$^+$ colorectal cancer stem cells. Tumour Biol. 2017; 39: 1010428317715155.
32. Dylla SJ, Beviglia L, Park IK, Chartier C, Raval J, Ngan L, et al. Colorectal cancer stem cells are enriched in xenogeneic tumors following chemotherapy. PLoS One. 2008; 3: e2428.
33. Lamprecht S, Schmidt EM, Blaj C, Hermeking H, Jung A, Kirchner T, et al. Multicolor lineage tracing reveals clonal architecture and dynamics in colon cancer. Nat Commun. 2017; 8: 1406.
34. Kreso A, Dick JE. Evolution of the cancer stem cell model. Cell Stem Cell. 2014; 14: 275-91.
35. Ricci-Vitiani L, Lombardi DG, Pilozzi E, Biffoni M, Todaro M, Peschle C, et al. Identification and expansion of human colon-cancer-initiating cells. Nature. 2007; 445: 111-5.
36. Hu Y, Xiao Q, Chen H, He J, Tan Y, Liu Y, et al. BEX2 promotes tumor proliferation in colorectal cancer. Int J Biol Sci. 2017; 13: 286-94.
37. Balko JM, Giltnane JM, Wang K, Schwarz LJ, Young CD, Cook RS, et al. Molecular profiling of the residual disease of triple-negative breast cancers after neoadjuvant chemotherapy identifies actionable therapeutic targets. Cancer Discov. 2014; 4: 232-45.
38. Morris A, Pagare PP, Li J, Zhang Y. Drug discovery efforts toward inhibitors of canonical Wnt/β-catenin signaling pathway in the treatment of cancer: a composition-of-matter review (2010-2020). Drug Discov Today. 2022; 27: 1115-27.
39. Liu L, Tao T, Liu S, Yang X, Chen X, Liang J, et al. An RFC4/Notch1 signaling feedback loop promotes NSCLC metastasis and stemness. Nat Commun. 2021; 12: 2693.
40. Lee SY, Jeong EK, Ju MK, Jeon HM, Kim MY, Kim CH, et al. Induction of metastasis, cancer stem cell phenotype, and oncogenic metabolism in cancer cells by ionizing radiation. Mol Cancer. 2017; 16: 10.
41. Kondo Y, Issa JP. Epigenetic changes in colorectal cancer. Cancer Metastasis Rev. 2004; 23: 29-39.
42. Yang L, Ma DW, Cao YP, Li DZ, Zhou X, Feng JF, et al. PRMT5 functionally associates with EZH2 to promote colorectal cancer progression through epigenetically repressing CDKN2B expression. Theranostics. 2021; 11: 3742-59.
43. Chen CY, Wu JJ, Lin YJ, Hsu CH, Hu JM, Chang PK, et al. Significance of hypermethylation of tumor-suppressor genes PTGER4 and ZNF43 at CpG sites in the prognosis of colorectal cancer. Int J Mol Sci. 2022; 23: 10225.
44. Jia M, Gao X, Zhang Y, Hoffmeister M, Brenner H. Different definitions of CpG island methylator phenotype and outcomes of colorectal cancer: a systematic review. Clin Epigenetics. 2016; 8: 25.
45. Zhang Z, Gao Y, Qian Y, Wei B, Jiang K, Sun Z, et al. The Lyn/RUVBL1 complex promotes colorectal cancer liver metastasis by regulating arachidonic acid metabolism through chromatin remodeling. Adv Sci (Weinh). 2025; 12: e2406562.
46. De Robertis M, Mazza T, Fusilli C, Loiacono L, Poeta ML, Sanchez M, et al. EphB2 stem-related and EphA2 progression-related miRNA-based networks in progressive stages of CRC evolution: clinical significance and potential miRNA drivers. Mol Cancer. 2018; 17: 169.
47. Wang TW, Chern E, Hsu CW, Tseng KC, Chao HM. SIRT1-mediated expression of CD24 and epigenetic suppression of novel tumor suppressor miR-1185-1 increases colorectal cancer stemness. Cancer Res. 2020; 80: 5257-69.
48. Huang R, Wang G, Song Y, Tang Q, You Q, Liu Z, et al. Colorectal cancer stem cell and chemoresistant colorectal cancer cell phenotypes and increased sensitivity to Notch pathway inhibitor. Mol Med Rep. 2015; 12: 2417-24.
49. Palle K, Mani C, Tripathi K, Athar M. Aberrant GLI1 activation in DNA damage response, carcinogenesis and chemoresistance. Cancers (Basel). 2015; 7: 2330-51.

Cite this article as: Qian Y, Wei J, Bian Y, Tan Y, Fang Y, Chen L, et al. BEX2 influences the MCL1-Hedgehog signaling axis to regulate the potential of stemness characterization in colorectal cancer. Cancer Biol Med. 2026; 23: 276-293. doi: 10.20892/j.issn.2095-3941.2025.0120